



# The water mass transformation framework and variability in hurricane activity

Elizabeth A. Harris<sup>1,2</sup> · Robert Marsh<sup>1</sup> · Jeremy. P. Grist<sup>3</sup> · Gerard. D. McCarthy<sup>4</sup>

Received: 10 July 2021 / Accepted: 24 January 2022 / Published online: 13 April 2022  
© The Author(s) 2022

## Abstract

Hurricane activity has been higher since 1995 than in the 1970s and 1980s. This rise in activity has been linked to a warming Atlantic. In this study, we consider variability of the volume of water warmer than 26.5 °C, considered widely to be the temperature threshold crucial to hurricane development. We find the depth of the 26.5 °C isotherm better correlated with seasonal hurricane counts than SST in the early part of the Atlantic hurricane season in some regions. The volume of water transformed by surface heat fluxes to temperatures above 26.5 °C is directly calculated using the Water Mass Transformation framework. This volume is compared with the year-to-year changes in the volume of water of this temperature to see how much of the volume can be explained using this calculation. In some years, there is notable correspondence between transformed and observed volume anomalies, but anomalies in other years must be largely associated with other processes, such as the divergence of horizontal heat transport associated with the AMOC. This technique provides evidence that, in a given year, coordinated physical mechanisms are responsible for the build-up of anomalous ocean heat; not only net surface heat exchange but also the convergence of horizontal heat transport from ocean currents, to provide fuel for larger numbers of intense hurricanes.

**Keywords** Hurricane · Water mass transformation · Surface heat flux · Atlantic · Warm water anomalies

## 1 Introduction

Recent North Atlantic hurricane seasons have produced several high impact hurricanes, including Harvey, Irma, and Maria in 2017, Florence and Michael in 2018, and Dorian in 2019, which resulted in 335 billion USD damage and over 3000 deaths (NCEI 2020). Questions remain open on drivers of high activity seasons. Variability in hurricane activity on a range of timescales has been linked to large scale climate oscillations, including the Atlantic Multidecadal Oscillation (AMO) (Goldenberg et al. 2001), or Atlantic Multidecadal Variability (AMV) (Zhang and Delworth 2006), the El Niño

Southern Oscillation (ENSO), the North Atlantic Oscillation (NAO) (Elsner and Jagger 2004), the Quasi-Biennial Oscillation (QBO) (Gray 1992), as well as variations in atmospheric aerosols (Evan et al. 2009), including dust (Wang 2012), volcanic emissions (Birkel et al. 2018), and pollution (Watanabe and Tatebe 2019).

On interannual timescales, the Atlantic hurricane season is subject to variable atmospheric processes. For example, Atlantic hurricane variability is negatively correlated with El Niño indices, as anomalously warm tropical Pacific Sea Surface Temperatures (SSTs) result in higher than average vertical wind shear in the tropical Atlantic, which inhibits vertical motion necessary for Atlantic hurricane formation (DeMaria 1996). On timescales longer than interannual, slower modes of ocean variability are important. Associated with warmer ocean temperatures in the tropical North Atlantic is an increase in available energy in the upper ocean to fuel hurricane development (Shapiro and Goldenberg 1998).

Much attention has focused on the role of oceanic warmth as a driver of Atlantic hurricane seasons, on a range of timescales. SST has been found to be more highly correlated with hurricane intensification than thermocline

✉ Elizabeth A. Harris  
e.harris@soton.ac.uk

<sup>1</sup> School of Ocean and Earth Science, University of Southampton, Southampton, UK

<sup>2</sup> Ariel Re, Hamilton, Bermuda

<sup>3</sup> National Oceanography Centre, Southampton, UK

<sup>4</sup> ICARUS, Department of Geography, Maynooth University, Maynooth, Co. Kildare, Ireland

depth over most of the North Atlantic (Balaguru et al. 2013). However, it is likely that in some regions, the volume of potentially hurricane-producing water may be a more physically meaningful metric than area-averaged SST. For example, intensity estimates of tropical cyclones around Bermuda were improved by use of subsurface temperatures rather than SST alone (Hallam et al. 2021).

Other investigations have found a meaningful role for aerosol concentration in multidecadal warming of the North Atlantic. This result has been simulated in climate modelling studies (Booth et al. 2012) due to variation in anthropogenic aerosols, and point to an influence on tropical cyclone activity (Dunstone et al. 2013). A modelled increase in anthropogenic sulphate aerosols can explain much of the observed cool period in the 1970s and 80s in the North Atlantic (Watanabe and Tatebe 2019). Mann et al. (2021) now suggest that multidecadal variability in Atlantic SST is mainly driven by volcanic activity, and finds no evidence for internal variability.

Rather than suggesting large-scale physical mechanisms for heat transfer into the ocean, this study directly quantifies the contribution of surface heat flux ( $Q_{net}$ ) processes to the variability of warm water volume available for hurricane development through the holistic Water Mass Transformation (WMT) framework (Groeskamp et al. 2019). The volume of water transformed across isotherms through  $Q_{net}$  is calculated using WMT. Accumulated transformation fluxes over a time interval are compared with observed changes in volume of water above a temperature threshold over the same interval.

This approach has the advantage of referencing the total volume of water above a temperature threshold intimately connected with hurricane development, 26.5 °C (McTaggart-Cowan et al. 2015), geographically confined to the Atlantic. This removes limits of fixed latitude and longitude, as for the conventional Main Development Region (MDR) for Atlantic hurricanes (Goldenberg et al. 2001), generally defined as 10–20°N, 20–80°W.

Oceanic conditions which sustain hurricane winds are not constrained to the MDR. In particular, warm water availability outside this region is one factor which could result in major hurricane landfall further north. Wang et al. (2011) investigated the areal extent of the Atlantic Warm Pool (AWP) and correlation with hurricane activity, emphasizing the importance of the AWP to the west of the MDR, extending across the Caribbean and the Gulf of Mexico. In summary, we quantify AWP volume anomalies attributed to anomalous air-sea interaction, with residual AWP volume anomalies attributed to a combination of mixing and advection.

The rest of the paper is organized as follows. In Sects. 2 and 3, we outline the WMT framework used in temperature space, and the datasets used here. In Sect. 4, we present our

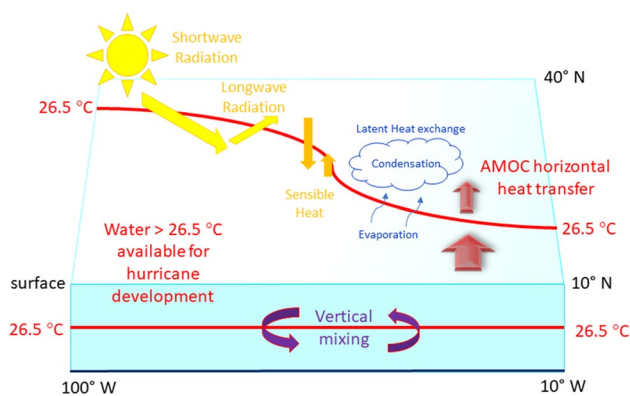


**Fig. 1** Heat transfer mechanisms leading to water warmer than 26.5 °C, critical to hurricane development, in the region southwards and upwards of thick red lines

results, starting with an overview of changes in the volume of warm water and hurricane activity over the last 40 years. We then outline the WMT at temperatures relevant to hurricane formation. Using this approach, we attribute changes in the volume of warm tropical waters directly to anomalous surface fluxes, and further consider the extent to which anomalous surface fluxes drive enhanced warm water volume in specific years, when hurricane activity was particularly intense. In Sect. 5, we conclude with a discussion of the extent to which our findings inform the wider efforts to associate active hurricane seasons with a warming tropical Atlantic.

## 2 Methods

In this section, the calculations used to quantify the volume of water warmer than 26.5 °C, generated from net surface heat flux using the WMT framework, are described. Returning to the original formulation of Walin (1982), the WMT framework (Groeskamp et al. 2019) can be applied in temperature space, quantifying volume fluxes across isotherms which are associated with variations of heat fluxes in that property space.

The net surface heat flux,  $Q_{net}$ , combines radiative processes with turbulent fluxes. Shortwave ( $Q_{sw}$ ) radiation is absorbed from the sun and net longwave ( $Q_{lw}$ ) radiation is obtained by balancing upwelling and downwelling heat fluxes. Sensible heat ( $Q_{sh}$ ) is transferred directly between the ocean surface and the atmosphere, and latent heat ( $Q_{lh}$ ) flux transfer results from evaporation, which cools the ocean, and condensation, which transfers heat into the ocean. These processes are depicted schematically in Fig. 1, for a region warmer than 26.5 °C in the North Atlantic, along with heat transfer by vertical mixing and ocean currents, such as those associated with the Atlantic Meridional Overturning

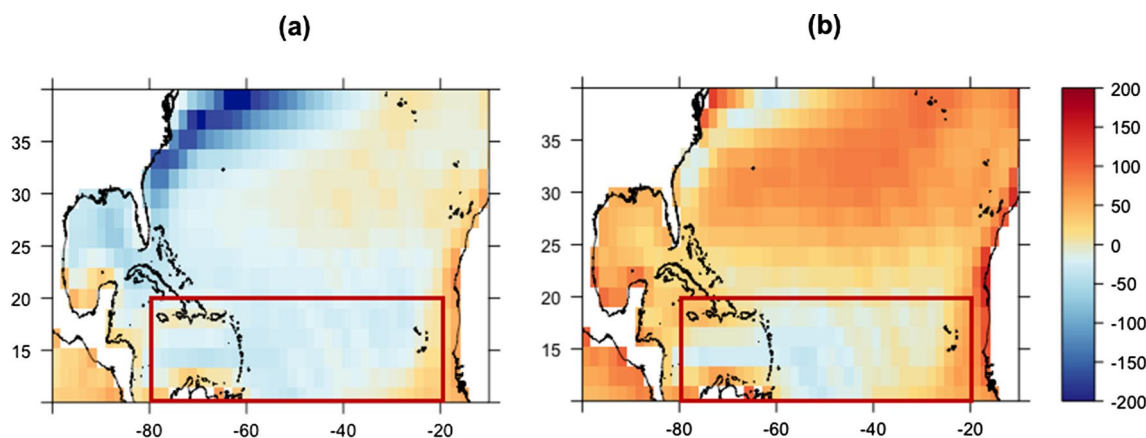


Fig. 2 NCEP 1980–2019 Mean  $Q_{net}$  ( $Wm^{-2}$ , positive into the ocean), MDR outlined in red: a Jan-Dec, b Apr-Sept

Circulation (AMOC). Throughout this study, our convention is that heat flux components are positive into the ocean, hence the net surface heat flux follows as:

$$Q_{net} = Q_{sw} + Q_{lw} + Q_{sh} + Q_{lh} \tag{1}$$

In Fig. 2, we show the long-term annual and April-September mean  $Q_{net}$ , across the tropical and subtropical North Atlantic. In most months, heat is lost to the atmosphere from the warm tropical surface waters of the MDR, particularly through the winter. The annual-mean heat flux is consequently negative across most of the MDR (Fig. 2a), although there is some net warming during April-September, most notably in the eastern MDR (Fig. 2b). It follows that years with less heat loss from the ocean, through these processes, will result in more water being transformed to warmer temperatures which can support potential hurricane development.

Groeskamp and Iudicone (2018) discuss the influence of  $Q_{sw}$  depth penetration for WMT due to the redistribution of heat with depth. In relation to local optical properties (notably related to the local concentration profile of chlorophyll-a) and thermal stratification, a small percentage of shortwave radiation will be absorbed at slightly lower temperatures. However, accounting for typical chlorophyll-a levels and globally averaging, they estimate that only around 3.3% of shortwave radiation is absorbed below the mixed layer. Even given relatively shallow mixed layer depths in our region of interest—from a summer minima of typically 20 m to a maxima of around 40 m in the eastern tropics and around 100 m in the western tropics (Holte et al. 2017)—this percentage is apparently also small across the tropical Atlantic, where 2–6% of shortwave radiation is absorbed below the mixed layer. We therefore adopt the conventional approach (Grist et al. 2014) of assuming all net  $Q_{sw}$  is absorbed at the surface, with negligible shortwave transmission and absorption beneath the surface. The calculated

change in water mass volume is thus associated with the net heating of the surface in the region of interest.

The volume of water transformed across isotherms by  $Q_{net}$  is calculated over the North Atlantic, north of 10°N, where there is sufficient Coriolis force for tropical storm spin up. Firstly, the diathermal temperature flux,  $Q_{in}(T)$  ( $^{\circ}C m^3 s^{-1}$ ) (2), is found by area-integrating  $Q_{net}$ , where SST is at or above a given value of temperature,  $T$ , then dividing by reference density,  $\rho_o$ , and specific heat capacity,  $c_p$ , where that isotherm is outcropped.

$$Q_{in}(T) = \frac{1}{\rho_o c_p} \int_{x_w}^{x_e} \int_{y_s}^{y_n} Q_{net}(x, y) \Gamma(SST(x, y), T) dx dy \tag{2}$$

where  $x, y$  are distance in west ( $w$ ) to east ( $e$ ) and south ( $s$ ) to north ( $n$ ) directions, integrating from a west limit ( $x_w$ ) to an east limit ( $x_e$ ), and from a south limit ( $y_s$ ) to a north limit ( $y_n$ ), and  $\Gamma$  is a sampling function;  $\Gamma = 1$  where  $SST > T$ , otherwise  $\Gamma = 0$ ;  $Q_{net}$  values at the selected temperatures are found using bilinear interpolation between both latitude and longitude points of the gridded data at each depth level. The diathermal temperature flux is proportional to the heat flux across a selected isotherm but constructed as a temperature flux to obtain a diathermal volume flux, as outlined below.

The diathermal volume flux, or thermal water mass transformation rate,  $F_T(T)$  ( $m^3 s^{-1}$ ), can then be arrived at by taking differences between  $Q_{in}(T)$  across two temperature surfaces.

$$F_T(T) = \frac{Q_{in}(T - \Delta T/2) - Q_{in}(T + \Delta T/2)}{\Delta T} \tag{3}$$

where  $Q_{in}$  is calculated at temperature intervals of  $\Delta T$ . This transformation rate is equivalent to rate of change of the volume of water with temperature exceeding  $T$ .

In this way, the volume of water transformed via surface heat fluxes across a particular temperature threshold can be calculated for each month. Other processes playing

a role in WMT are considered as the residual of observed volume anomalies after water transformed by surface heat fluxes is accounted for. An additional advantage of the WMT framework is that changes in water mass properties can be analysed without the limitations of an arbitrary reference temperature otherwise used in the calculation of Ocean Heat Content (Holmes et al. 2019).

### 3 Data

The National Center for Environmental Prediction/National Center for Atmospheric Research (NCEP/NCAR) reanalysis (Kalnay et al. 1996) is used for monthly mean values of heat transfer from the atmosphere into the ocean from 1980 through 2019 in order to calculate  $Q_{net}$  anomalies. Wind speed and cloud cover values used in further analysis are also from this source. Incorporating all available observational data, the reanalysis product consists of data at 2.5° horizontal resolution from 1950 onwards. Previous similar uses of this reanalysis data in the WMT framework include studies of the subtropical and subpolar North Atlantic (Grist et al. 2014).

The NCEP Global Ocean Data Assimilation System (GODAS) ocean reanalysis product (Behringer and Xue, 2004) contains gridded global potential temperature at 40 discrete depths, at 1/3° latitude and 1° longitude spacing, from 1980 to present. It is important to note that observations assimilated into these products are increasingly scarce with depth and further back in time, so the degree of constraint afforded by the observations will vary in a corresponding manner. GODAS potential temperatures are used to calculate observed volume anomalies of water warmer than 26.5 °C.

The US National Hurricane Center (NHC) tropical cyclone data, HURDAT, was used to obtain annual hurricane counts and location of the onset of hurricane force winds. This dataset includes storm center coordinates and maximum winds at 6 hourly intervals over the ocean. These wind speeds are rounded to the nearest 5 knots. This data has been incorporated in a global tropical cyclone dataset in a standard format, maintained by the International Best Track Archive for Climate Stewardship (IBTrACS) (Knapp et al. 2010, Knapp et al. 2018).

Ocean heat transport across 26.5°N from the RAPID-MOCHA array 2004–2018 (Cunningham et al. 2007, Kanzow et al. 2009) is comprised of 4 components. Gulf Stream transport is measured by the amount of electrical current generated by flow across an underwater cable which runs between Florida and the Bahamas. Ekman transport is derived from satellite scatterometer surface wind observations. The southward mid ocean transport is calculated using current meters at shallower depths. Further down the water

column, current is calculated from temperature and salinity measurements at various depths by zonally integrating the geostrophic profile. Instruments are attached to a variety of deep-water moorings spanning 26.5°N.

## 4 Results

We first summarise the extent to which warm water volume and hurricane activity have co-varied since 1980. We then introduce the WMT framework in temperature space, applied to the warm water pool. Over our study period, we present evidence of a leading role for surface fluxes as the dominant driver of anomalous upper ocean warmth in several years of the last four decades.

### 4.1 Warm water volume and hurricane activity

North Atlantic hurricane activity has generally been above the 1970–2019 average of 6.2 hurricanes per year since 1995, with an average of 7.5 hurricanes per year 1995–2019. This is 50% higher than the mean of 5 hurricanes per year during 1970–1995 (Fig. 3). In only 6 of the 25 years during 1995–2019 was annual hurricane activity below the 1970–2019 mean, aligned with the GODAS volume anomalies zero-line in Fig. 3. Recent years with the highest annual hurricane counts include 2005 and 2010. Anomalous volume of water warmer than 26.5 °C in the North Atlantic shows similar multidecadal variability, with warm episodes becoming more frequent after 1995. While the most active years don't always occur when the volume of water warmer than 26.5 °C is highest, due to, for example, the important role of vertical wind shear (DeMaria 1996), active years have become more frequent during this recent regime of a larger volume of warm water. The annual average anomalous volume water warmer than 26.5 °C is positively correlated with annual Atlantic hurricane count, with a Pearson correlation coefficient of 0.42, statistically significant at the 99% level.

The relationship between Atlantic SST and seasonal hurricane counts is well established (Goldenberg et al. 2001; Gray et al. 1992; Wang et al. 2012). Rather than SST, we however find better correlation between the depth of the 26.5 °C isotherm ( $Z_{26.5}$ ) at each grid point with North Atlantic basin seasonal hurricane count, in some regions of the North Atlantic in the spring. This is most clearly seen in April (Fig. 4a), focussed in the tropics at 60°W. These correlations are significant at the 95% level, as indicated by stippling on the plots. This finding is in line with studies which highlight the importance of Ocean Heat Content as a hurricane intensity forecasting tool (Mainelli et al. 2008).

Local SST correlation patterns with seasonal basin hurricane count show the typical horseshoe shape of AMV, particularly by May (Fig. 4d). Areas of deep warm water in

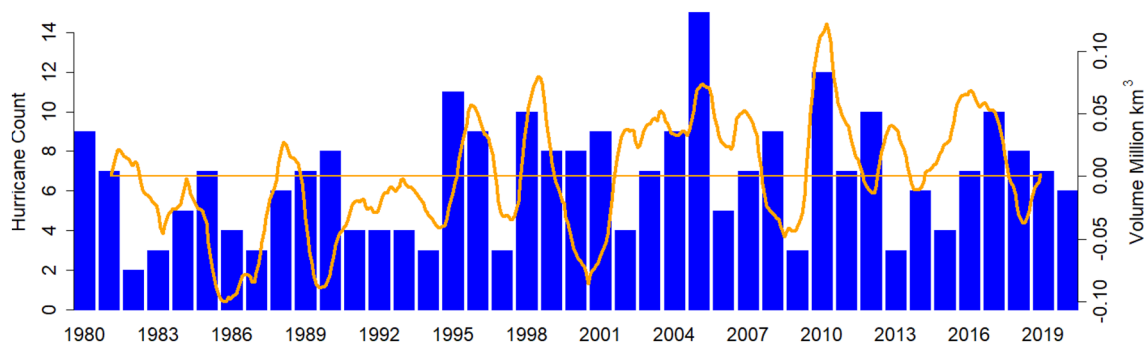


**Fig. 3** HURDAT Annual North Atlantic Hurricane count (blue bars) and GODAS volume anomalies of water warmer than 26.5 °C in the Atlantic north of 10° N 1980–2019, applying 12-month centred mov-

ing average (orange line). For GODAS volume anomalies, the zero-line is aligned with the mean hurricane count

the spring indicate water warm enough to sustain tropical development early in the Atlantic hurricane season, which is likely to increase total hurricane count for the year by adding early season storms and suggests a deeper pool of warm water will be available later in the season.

These correlations were examined in detail to see if better correlation existed between early season hurricane count (hurricanes forming before July 1) and 26.5 °C isotherm depth in a particular month (April or May for example), than hurricane counts for the whole season, but that did not seem to be the case. This observation implies that early season hurricanes are not driving the correlation. As the sample size of these hurricanes since 1980 is quite small (8 hurricanes), it is unlikely that a high correlation would be observed. Indeed, some of these storms are generated from unusual atmospheric conditions rather than underlying oceanic heat. One example is Hurricane Alex, which formed in January 2016 from an extra-tropical low (Jesús González-Alemán, 2018).

## 4.2 Characteristics of water mass transformation

Surface WMT calculates the rate that water masses are transformed across isotherms by heat transfer between the ocean and the atmosphere. A North Atlantic WMT climatology shows the transformation rate across all isotherms found in the North Atlantic, from 0 to 31 °C (Fig. 5). The climatology is consistent with annual net cooling and warming in different temperature ranges. Surface water is transformed by  $Q_{net}$  across isotherms: towards cooler temperatures in the range 0 to 27 °C, where  $Q_{net} < 0$ ; towards higher temperatures between 27 and 30 °C, where  $Q_{net} > 0$ . The latter temperatures are of particular relevance to hurricane and major hurricane development. This indicates that in general, local surface fluxes act to increase the volume of water warmer than 27 °C.

In general, WMT produces distinct water masses via either warming or cooling while other processes act in the opposite sense to mix or homogenize the distribution in Fig. 5. Transports across lateral boundaries (in particular 10°N) import and export water masses in different temperature ranges. Vertical mixing by sub-mesoscale eddies distributes heat down the water column (Hieronymus et al. 2014; Holmes et al. 2019), to depths inaccessible for hurricane development. Heat is also advected poleward with the large-scale ocean circulation, into cooler regions of the North Atlantic. A portion of the air-sea heat flux into the tropical ocean is thus redistributed by mixing and advected poleward, reducing the volume of warm water generated by WMT.

Considering water temperatures affecting hurricane development, annual average cumulative transformed water volume of temperatures warmer than 26.5 °C peaks in August. This leads actual warm water volume, which peaks in September (Fig. 6), over the 1980–2019 time period. This is consistent with atmosphere–ocean heat exchange being a critical process in forming these warm waters. We note that in a case where the surface fluxes are solely responsible for the volume variability, then actual volume anomaly would equal the time-integral of the transformation rate.

The net surface heat flux,  $Q_{net}$  transforms water from cooler SST to water warmer than 26.5 °C under the hurricane genesis and track regions through the spring and summer months. Figure 7a plots climatological  $Q_{net}$  during 1980–2019 transferred into the ocean, time-integrated from April to September, where SST exceeds 26.5 °C—the integrand of Eq. 2, where  $T=26.5$  °C. While other processes also contribute to the observed September climatological depth of the 26.5 °C isotherm in the North Atlantic (Fig. 7b), spatial coherence between the area which can be transformed to temperatures warmer than 26.5 °C through the spring and early summer, and the observed climatological area of 26.5 °C waters in September is suggested by comparison

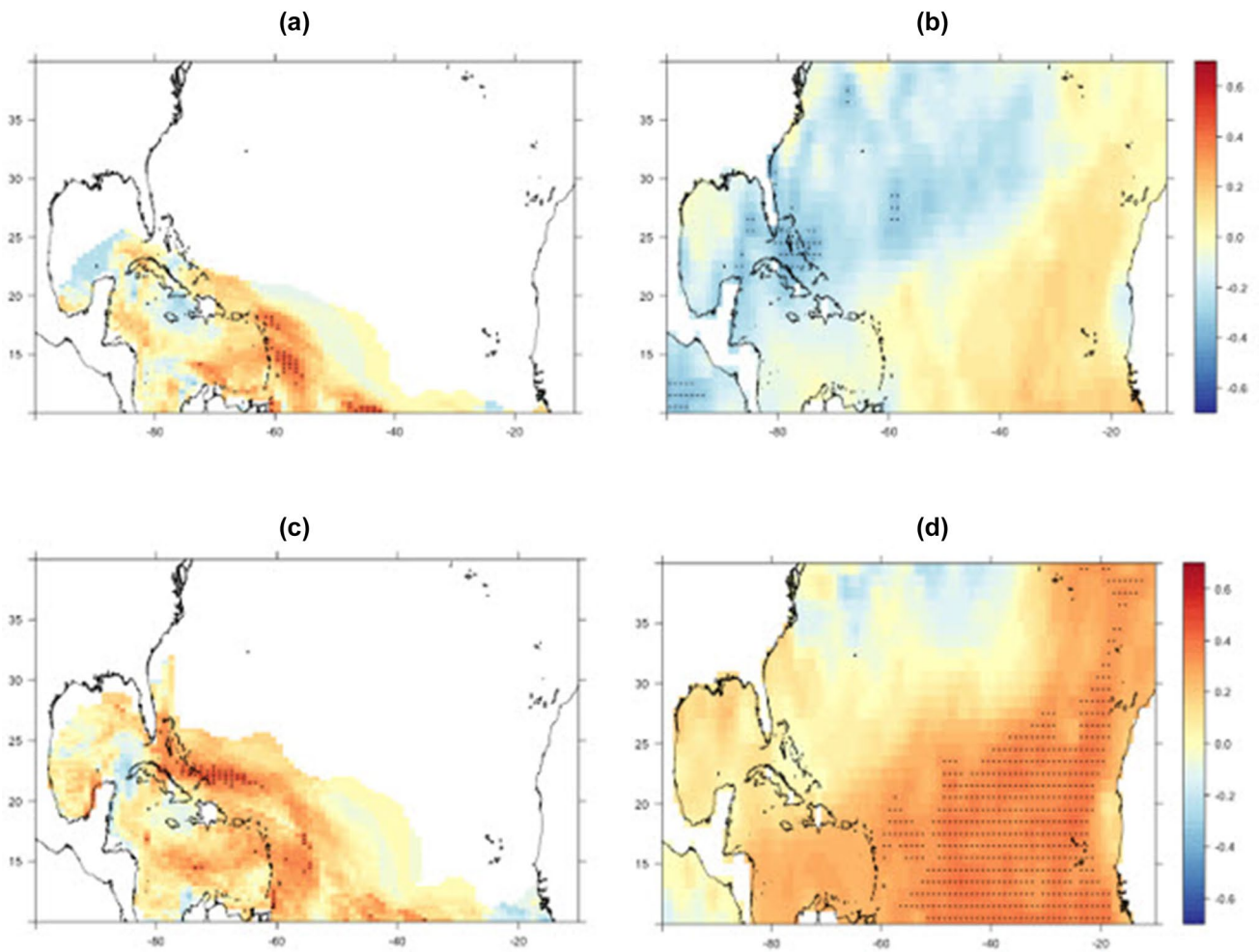


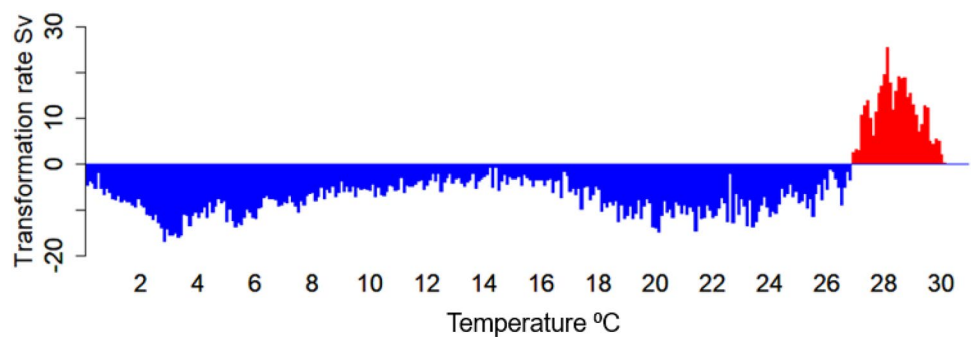
**Fig. 4** Pearson correlation coefficient between Atlantic basin seasonal hurricane count 1980–2019 and depth of the 26.5 °C isotherm in different months: **(a)**  $r(Z_{26.5}, \text{hurricane count})$ , April; **(b)**  $r(\text{SST}, \text{hurricane count})$ , April; **(c)**  $r(Z_{26.5}, \text{hurricane count})$ , May; **(d)**  $r(\text{SST}, \text{hurricane count})$ , May. Stippling indicates 95% significance level

cane count), April; **(c)**  $r(Z_{26.5}, \text{hurricane count})$ , May; **(d)**  $r(\text{SST}, \text{hurricane count})$ , May. Stippling indicates 95% significance level

between these two plots. Relating this more closely to hurricane development metrics, the point at which 1980–2019 tropical cyclones strengthened into hurricanes with maximum sustained 1-min mean winds of 64 knots or greater is overlaid onto the climatological depth of the 26.5 °C isotherm. These points are found south of 40°N, west of

40°W and south of 20°N, east of 40°W, and are bounded to the south around 10°N. Few points are found north of this region of the North Atlantic, providing additional observational evidence to connect this water mass with hurricane development. The patterns of strong net warming and 26.5 °C isotherm depth, which span the breadth of the

**Fig. 5** Annual-mean transformation rate (Sv) for the Atlantic north of 10°N as a function of SST 1980–2019, given diathermal temperature fluxes at 0.25 °C intervals; positive values imply transformation of water towards higher temperatures has occurred over the period



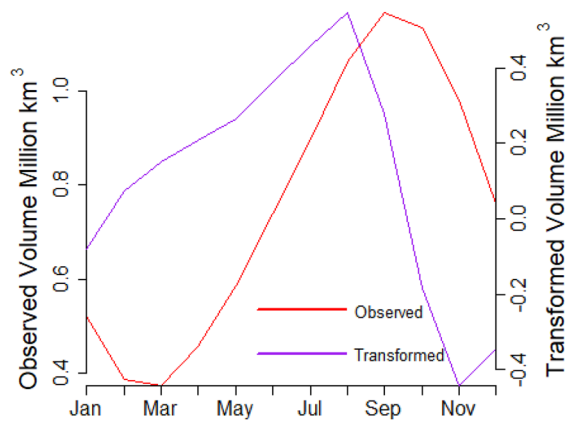


**Fig. 6** 1980–2019 mean monthly volume transformed across 26.5 °C isotherm (purple, right axis) and actual volume warmer than 26.5 °C (red, left axis) (million km<sup>3</sup>)

Atlantic basin and extend to ~40°N, reinforce our emphasis that ocean warming of consequence for hurricane genesis is not confined to the MDR.

### 4.3 Inferred warm water volume changes

In Fig. 8, time series of GODAS 1980–2019 differences from one month to the next of observed volume anomalies

of water warmer than 26.5 °C are plotted with NCEP-NCAR anomalous monthly transformation rate across 26.5 °C, both expressed as million km<sup>3</sup> per month. The aim is to see how closely these may be linked, and how  $Q_{net}$  processes may therefore drive development of this warm water to fuel hurricanes, and, by inference, the extent to which other processes must contribute to form this water mass. Monthly anomalies of water transformed by  $Q_{net}$  are positively correlated with month-to-month actual volume change anomalies of water warmer than 26.5 °C (Fig. 8). The Pearson correlation coefficient is 0.32, which is statistically significant at the 99% confidence level.

However, while the correlation is significant, it is also clear that the level of agreement between WMT and the observed warm water volume exhibits marked temporal variability. In particular, there is close correspondence between the two time series during several periods. One such period was 1998, when there was a notable peak in both time series, and the transformation rate led the observed volume change of water warmer than 26.5 °C by a few months. This also coincided with the beginning of the multi-decadal (post-1998) period of above-average warm water volume available for hurricane development. Examining 1998 in more detail, in most months there was anomalously positive transformation, but this was particularly marked during June through

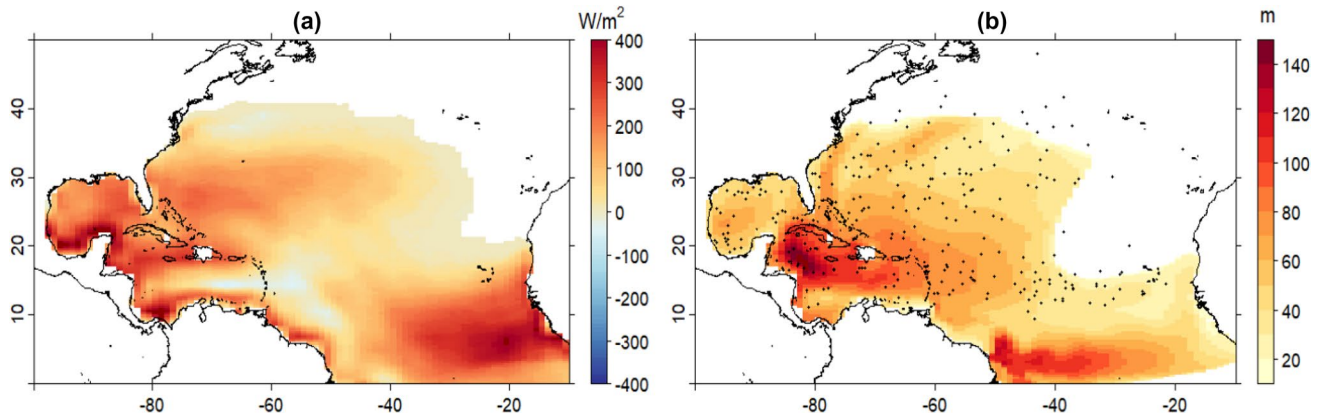


**Fig. 7** **a** Mean 1980–2019 April-September  $Q_{net}$  ( $Wm^{-2}$ ) into the ocean where SST exceeds 26.5 °C, **b** 1980–2019 September mean depth of 26.5 °C isotherm (m) with HURDAT 1980–2019 hurricane formation points overlaid)

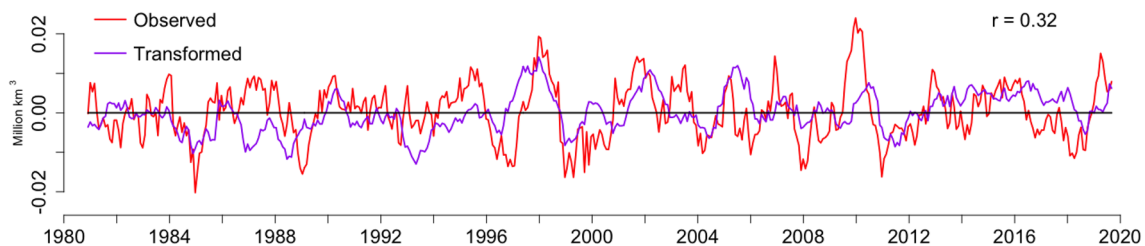
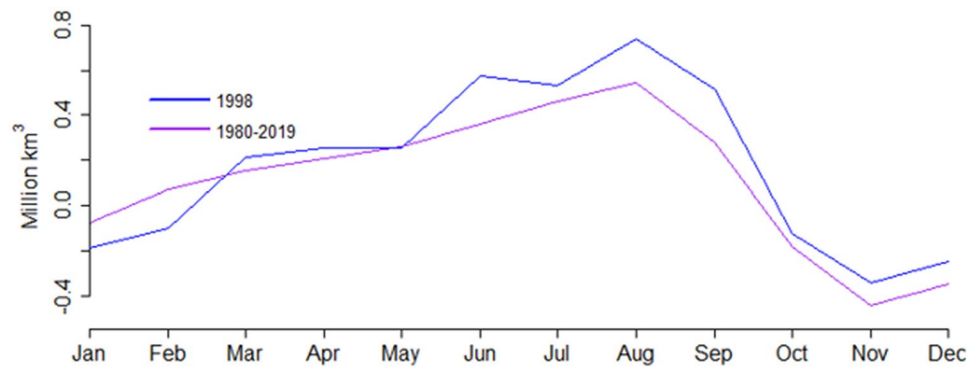


**Fig. 8** Anomalous observed month-to-month (red) volume change of water warmer than 26.5 °C and the anomalous transformation rate (million km<sup>3</sup> per month) across the 26.5 °C isotherm (purple), applying 12-month centred moving average

**Fig. 9** 1980–2019 (blue) annual cycle of volume transformed across 26.5 °C isotherm (million km<sup>3</sup>) versus climatology (purple)



September (Fig. 9). This is important as it highlights that surface fluxes during as well as before the hurricane season can be important in driving anomalies in warm water volume.

In Fig. 10, we show anomalies of monthly  $Q_{net}$  over waters warmer than 26.5 °C for June to September of 1998, relative to 1980–2020 climatological values. These positive anomalies led to anomalous warm water transformation during these peak months of the 1998 hurricane season.

In 1998, hurricane activity was well above average (Pasch et al. 2001), with an Accumulated Cyclone Energy (ACE) of 182, 67% higher than that of the 1980–2019 average ACE, and the 5<sup>th</sup> highest since 1970, when satellite data coverage extended basin-wide and this metric could be diagnosed appropriately (Kossin et al. 2007). Major Hurricanes Bonnie, Georges, and Mitch all made landfall in 1998. Anomalous net surface heating heavily contributed to this, the deadliest Atlantic Hurricane season in the last 200 years. The period during 1995–1998 of enhanced transformation appears to have also been important in sustaining a shift from below average to above average warm water volume that occurred near this time (Fig. 3).

By contrast, in other years, it is clear from the difference between the two signals in Fig. 8 that additional processes must have contributed to accumulation of warm waters. The warm water volume will further vary as a consequence of anomalies in heat transport divergence associated with both large-scale geostrophic currents and Ekman dynamics. In 2009–2010,  $Q_{net}$  fails to explain up to 0.015 million km<sup>3</sup> of anomalous volume of water warmer than 26.5 °C in a month. Bryden et al. (2014) calculate a 0.4 PW reduction in ocean heat transport across 26°N during this period. A decrease in the AMOC then allowed a greater accumulation of heat in the tropical Atlantic in this period, leading to a much greater volume of water warmer than 26.5 °C during the very active 2010 hurricane season.

The relative contributions of these heat sources will also vary on longer timescales over the study period. A downward trend has been observed in AMOC transport since 2008 in the RAPID array measurements at 26.5°N (Smeed et al. 2018) which would help develop anomalously larger

volume of warm North Atlantic water on a decadal timescale. Bryden et al. (2020) note a decrease of 0.17 PW across this latitude since 2009. Hallam et al. (2019) discuss the importance of this slowdown to the 2010 hurricane season in comparison with the 2017 hurricane season, where they show that weaker net heat loss to the atmosphere in the northeastern MDR was a driver of anomalously warm SST.

These differences between observed and transformed volume of warm water are plotted in Fig. 11 along with negative RAPID heat transport anomalies, suggesting the amount of heat retained in the tropical Atlantic. There is a correspondence between the anomalous residual warm water volume not explained by surface fluxes and the anomalous export of ocean heat from the tropics associated with AMOC variability, notably in 2009 and 2012. The Pearson correlation coefficient for the residual volume of water warmer than 26.5 °C after accounting for the volume transformed by  $Q_{net}$ , and annual mean RAPID heat flux anomalies is  $-0.60$ .

To be more specific about the physical processes behind  $Q_{net}$ , we examine anomalies in the four terms of the net heat flux (Eq. 1). To isolate the dominant component in heat flux variability for warm water in this region of the ocean, the transformation rate across the 26.5 °C isotherm was separately calculated for each component of  $Q_{net}$ . The transformation rate calculated with latent heat flux,  $Q_{lh}$  (Fig. 12) explains 35% ( $r=0.59$ ) of the transformation rate calculated using  $Q_{net}$  for this particular temperature threshold. In comparison, calculating the transformation rate with other components of  $Q_{net}$ , including  $Q_{lw}$  and  $Q_{sw}$  explains 3% (3% and less than 1% respectively) of the total variance. The transformation rate calculated with  $Q_{sh}$  is highly correlated ( $r=0.72$ ) with the total, but is an order of magnitude smaller, and so on its own contributes little to the WMT variability.

#### 4.4 Drivers of warm water volume changes

Having identified  $Q_{lh}$  as the main driver of anomalous transformation of water towards temperatures above 26.5 °C, the impact of the atmospheric conditions on latent heat exchange into the ocean are now considered. Heat is gained by the ocean when there is a lower rate of evaporation or



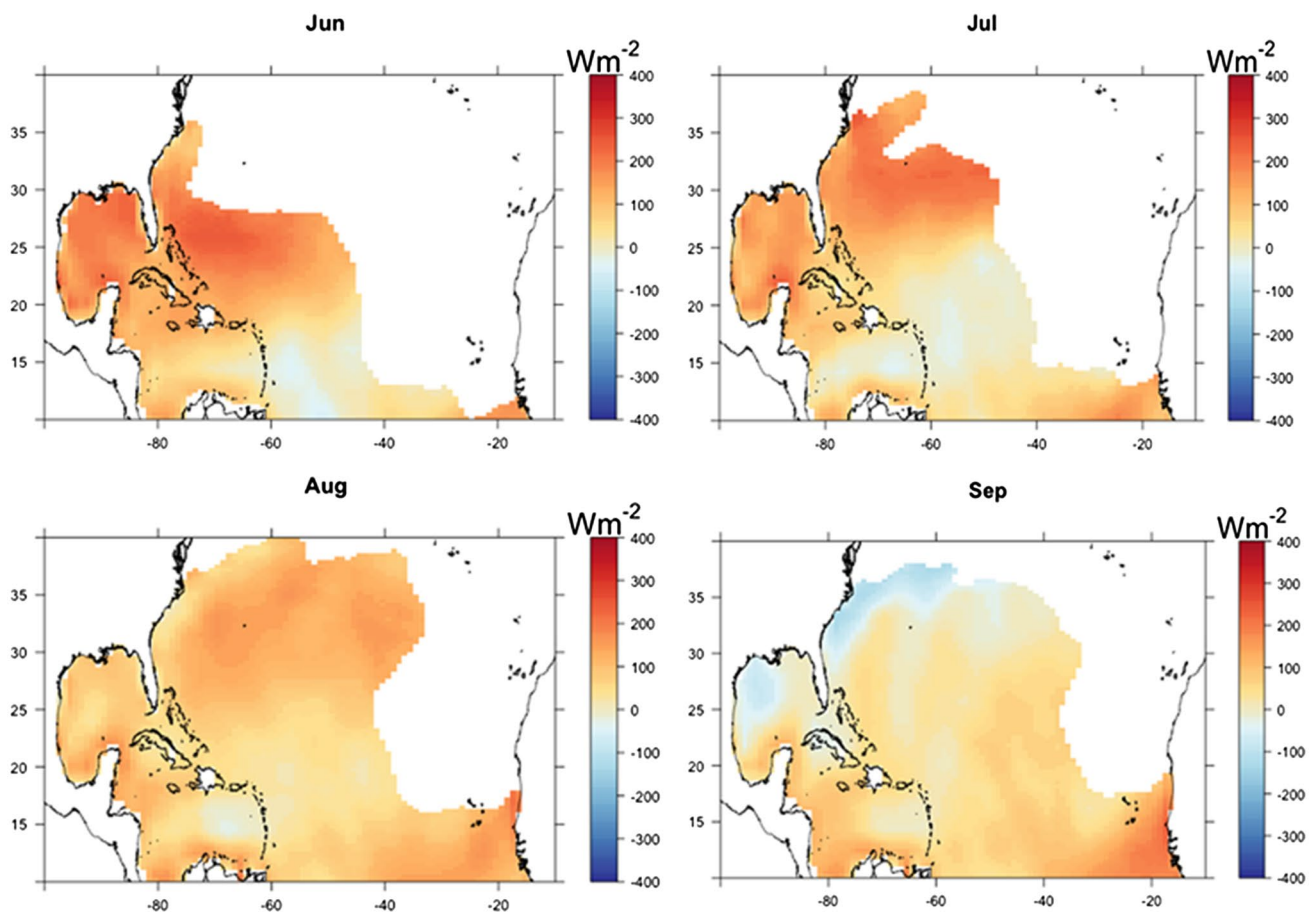


Fig. 10 Anomaly of June–September  $Q_{net}$  ( $Wm^{-2}$ ) in 1998 where SST > 26.5 °C

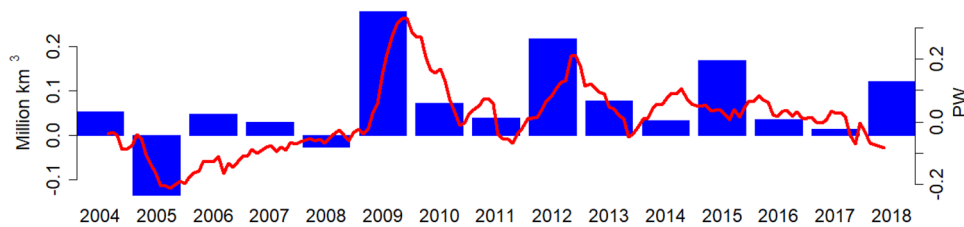


Fig. 11 Difference in 4-month warm water volume anomalies (Blue) between observed (EN4) July to October volume anomalies > 26.5 °C and that inferred by the anomalous integrated May to August trans-

formation across the 26.5 °C isotherm, with negative RAPID heat transport anomalies across 26°N (red), applying 12-month centred moving average

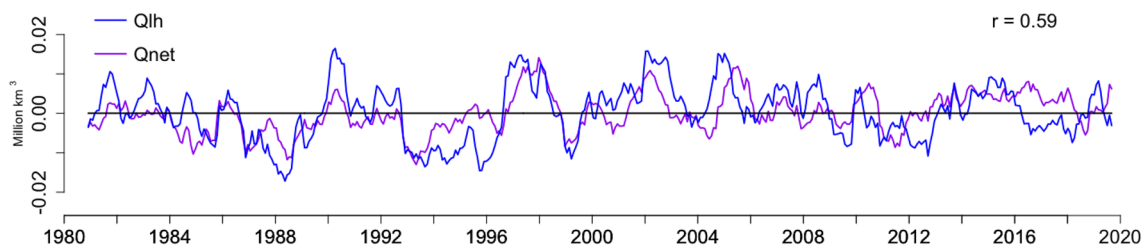


Fig. 12 Transformation rate anomalies (units: million of  $km^3$  per month) across the 26.5 °C isotherm calculated from  $Q_{net}$  (purple) and  $Q_{lh}$  (blue), applying 12-month centred moving average

less latent heat flux to the atmosphere. In Fig. 13, we plot the local correlation coefficient between  $Q_{lh}$  and wind speed (Fig. 13a) and cloud cover (Fig. 13b). Conditions conducive to a low evaporation rate and reduced latent heat loss include high surface humidity and light winds.  $Q_{lh}$  is negatively correlated to a larger degree ( $r < -0.5$ ) with wind speed across the majority of the hurricane MDR, and cloud cover in the eastern MDR (Fig. 13), implying that weaker winds lead to reduced latent heat loss and an increase of net heat flux into the ocean. Figure 13b however, implies that enhanced latent heat loss is associated with increased cloudiness. This relationship suggests that whereas latent heat flux variability is likely to be influenced by wind speed variations, cloud cover variability is more likely to respond to it. These conditions have been found to strengthen under a positive phase of tropical AMV (Bellomo et al. 2016).

## 5 Conclusions

Multidecadal hurricane activity is largely associated with anomalously warm water in the tropical and subtropical North Atlantic. We have applied the WMT framework (Groeskamp et al. 2019) in temperature space to quantify the volume of water transformed at the surface through air-sea interaction, attributed to the net surface heat flux,  $Q_{net}$ . It is shown that the amount of water warmer than  $27\text{ }^{\circ}\text{C}$  has increased in the last 40 years, with the transformed volume of water warmer than  $26.5\text{ }^{\circ}\text{C}$  leading observed volume anomalies through the spring and early summer. The transformed volume of water warmer than  $26.5\text{ }^{\circ}\text{C}$  shows signs of spatial coherence with the observed volume, which is closely

tied to the area identified earlier, where storms are able to intensify into hurricanes.

Anomalous positive WMT increases the volume of warm water to the north and east of this hurricane development area. Wang et al. (2010) note that years where the Atlantic Warm Pool is larger than average have increased genesis further east and more re-curving tracks. While some of these tracks may remain over the open ocean, the chance of landfall in the US Northeast states is also likely to increase (Dailey et al. 2009). Similarly, Kossin et al. (2010) group Atlantic storms into clusters, finding that increasing trends in recent hurricane activity are driven by the storm clusters originating in the deep tropics. These storms make up the largest proportion of major hurricanes and also account for the majority of storms making landfall further north along the US coastline.

Transformation rate anomalies across  $26.5\text{ }^{\circ}\text{C}$  in the North Atlantic are highly variable on timescales from intra-seasonal to multidecadal. A time dependent fraction of this variability is attributed to  $Q_{net}$ , using the WMT framework to calculate monthly volume anomalies that can be compared with observed anomalies. We identify the active and deadly hurricane season of 1998 (Pasch et al. 2001) as a year with particularly close correspondence between transformed and observed volume anomalies of substantial magnitude.

The other major influences on intraseasonal variability of the warm water volume are likely anomalous ocean heat transport divergence, associated with changes in both the AMOC (Zhang et al. 2019, and references therein) and Ekman dynamics, both of which are related in turn to the same anomalous winds that modulate the turbulent surface fluxes. Heat transport changes associated with the

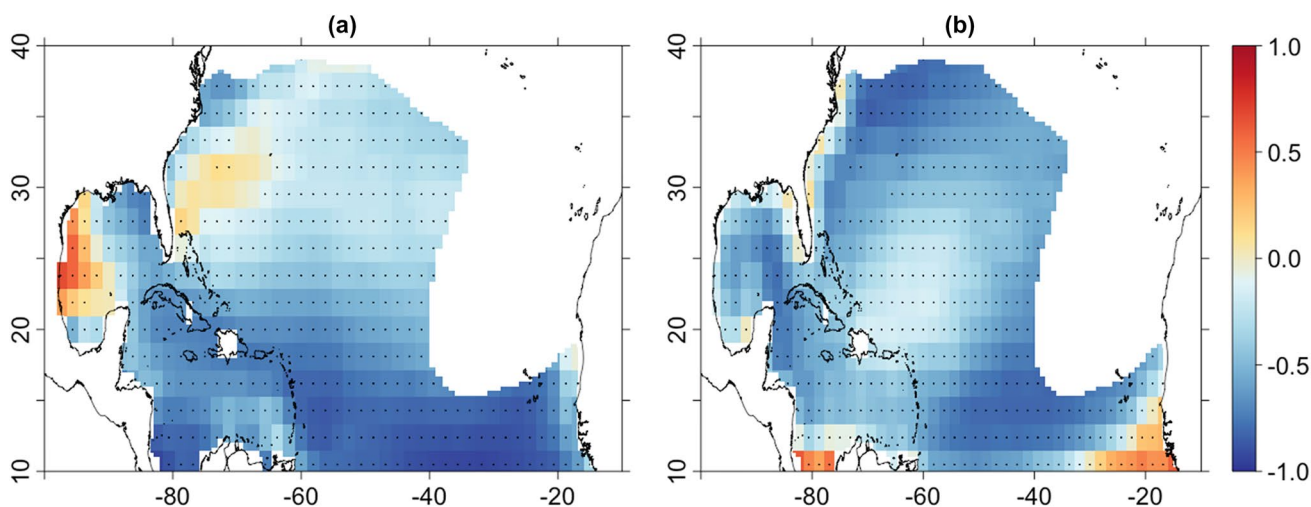


**Fig. 13** **a** Pearson correlation coefficient heat map for  $Q_{lh}$  and wind speed **b** correlation coefficient heat map for  $Q_{lh}$  and cloud fraction using NCEP-NCAR data spanning 1980–2019. Values are only plot-

ted where 1980–2019 September mean depth of  $26.5\text{ }^{\circ}\text{C}$  isotherm is greater than 10 m. Stippling indicates 95% significance level

30% AMOC downturn of 2010 account for the observed increase of warm water volume in that exceptional year.

This analysis, using the WMT framework, quantifies the amount of warm water available for hurricane development which is transformed, accounting for air-sea heat flux variability that is primarily related to surface winds. This mechanism only appears effective in some years, due to contribution in other years of variable heat transfer from ocean currents. This reinforces ideas that, at interannual and decadal timescales, coordinated physical mechanisms must come together to explain recent warming of the tropical North Atlantic which has been conducive to more intense hurricane seasons and more frequent landfalls of destructive storms.

**Acknowledgements** This analysis was possible due to the public availability of the NCEP/NCAR Reanalysis Monthly Means and Other Derived Variables data (<https://psl.noaa.gov/data/gridded/data.ncep.reanalysis.derived.surfaceflux.html>), the NCEP Global Ocean Data Assimilation System (GODAS) data (<https://psl.noaa.gov/data/gridded/data.godas.html>) and International Best Track Archive for Climate Stewardship (IBTrACS) data (<https://www.ncdc.noaa.gov/ibtracs/index.php?name=ib-v4-access>). We thank two anonymous reviewers for perceptive comments, helping us to substantially improve the manuscript.

**Funding** Ariel Re kindly provided funding for this project.

**Data availability** All data is publicly available.

**Code availability** Not applicable.

## Declarations

**Conflicts of interest** Not applicable.

**Open Access** This article is licensed under a Creative Commons Attribution 4.0 International License, which permits use, sharing, adaptation, distribution and reproduction in any medium or format, as long as you give appropriate credit to the original author(s) and the source, provide a link to the Creative Commons licence, and indicate if changes were made. The images or other third party material in this article are included in the article's Creative Commons licence, unless indicated otherwise in a credit line to the material. If material is not included in the article's Creative Commons licence and your intended use is not permitted by statutory regulation or exceeds the permitted use, you will need to obtain permission directly from the copyright holder. To view a copy of this licence, visit <http://creativecommons.org/licenses/by/4.0/>.

## References

- Balaguru K, Leung LR, Yoon JH (2013) Oceanic control of northeast Pacific hurricane activity at interannual timescales. *Environ Res Lett* 8(4):044009
- Behringer DW, Xue Y (2004) Evaluation of the global ocean data assimilation system at NCEP: The Pacific Ocean. In Proc. Eighth Symp. on Integrated Observing and Assimilation Systems for Atmosphere, Oceans, and Land Surface. Seattle, Wash: AMS 84th Annual Meeting, Washington State Convention and Trade Center.
- Bellomo K, Clement AC, Murphy LN, Polvani LM, Cane MA (2016) New observational evidence for a positive cloud feedback that amplifies the Atlantic Multidecadal Oscillation. *Geophys Res Lett* 43(18):9852–9859
- Birkel SD, Mayewski PA, Maasch KA, Kurbatov AV, Lyon B (2018) Evidence for a volcanic underpinning of the Atlantic multidecadal oscillation. *NPJ Clim Atmos Sci* 1(1):1–7
- Booth BB, Dunstone NJ, Halloran PR, Andrews T, Bellouin N (2012) Aerosols implicated as a prime driver of twentieth-century North Atlantic climate variability. *Nature* 484(7393):228–232
- Bryden HL, King BA, McCarthy GD, McDonagh EL (2014) Impact of a 30% reduction in Atlantic meridional overturning during 2009–2010. *Ocean Sci* 10(4):683–691
- Bryden HL, Johns WE, King BA, McCarthy G, McDonagh EL, Moat BI, Smeed DA (2020) Reduction in ocean heat transport at 26 N since 2008 cools the eastern subpolar gyre of the North Atlantic Ocean. *J Clim* 33(5):1677–1689
- Cunningham SA, Kanzow T, Rayner D, Baringer MO, Johns WE et al (2007) Temporal variability of the Atlantic meridional overturning circulation at 26.5°N. *Science* 317:935–938
- Dailey PS, Zuba G, Ljung G, Dima IM, Guin J (2009) On the relationship between North Atlantic Sea surface temperatures and U.S. Hurricane Landfall Risk. *J Appl Meteorol Climatol* 48:111–129
- DeMaria M (1996) The effect of vertical shear on tropical cyclone intensity change. *J Atmos Sci* 53(14):2076–2088
- Dunstone NJ, Smith DM, Booth BBB, Hermanson L, Eade R (2013) Anthropogenic aerosol forcing of Atlantic tropical storms. *Nat Geosci* 6(7):534–539
- Elsner JB, Jagger TH (2004) A hierarchical Bayesian approach to seasonal hurricane modeling. *Journal of Climate*, 17(14), 2813–2827.
- Evan AT, Vimont DJ, Heidinger AK, Kossin JP, Bennartz R (2009) The role of aerosols in the evolution of tropical North Atlantic Ocean temperature anomalies. *Science* 324(5928):778–781
- Goldenberg SB, Landsea CW, Mestas-Núñez AM, Gray WM (2001) The recent increase in Atlantic hurricane activity: causes and implications. *Science* 293(5529):474–479
- Good SA, Martin MJ, Rayner NA (2013) EN4: Quality controlled ocean temperature and salinity profiles and monthly objective analyses with uncertainty estimates. *J Geophys Res* 118(12): 6704–6716.
- Gray WM, Landsea CW, Mielke PW Jr, Berry KJ (1992) Predicting Atlantic seasonal hurricane activity 6–11 months in advance. *Weather Forecast* 7(3):440–455
- Grist JP, Josey SA, Marsh R, Kwon Y-O, Bingham RJ, Blaker AT (2014) The surface-forced overturning of the north atlantic: estimates from modern era atmospheric reanalysis datasets. *J Climate* 27:3596–3618. <https://doi.org/10.1175/JCLI-D-13-00070.1>
- Groeskamp S, Iudicone D (2018) The effect of air-sea flux products, shortwave radiation depth penetration, and albedo on the upper ocean overturning circulation. *Geophys Res Lett* 45(17):9087–9097
- Groeskamp S, Griffies SM, Iudicone D, Marsh R, Nurser AG, Zika JD (2019) The water mass transformation framework for ocean physics and biogeochemistry. *Ann Rev Mar Sci* 11(1):271–305
- Hallam S, Marsh R, Josey SA, Hyder P, Moat B, Hirschi JJM (2019) Ocean precursors to the extreme Atlantic 2017 hurricane season. *Nat Commun* 10(1):1–10
- Hallam S, Guishard M, Josey SA, Hyder P, Hirschi JJM (2021) Increasing tropical cyclone intensity and potential intensity in the subtropical Atlantic around Bermuda from an ocean heat content perspective 1955–2019. *Environ Res Lett*.

- Hieronymus M, Nilsson J, Nycander J (2014) Water mass transformation in salinity–temperature space. *J Phys Oceanogr* 44(9):2547–2568
- Holmes RM, Zika JD, England MH (2019) Diathermal heat transport in a global ocean model. *J Phys Oceanogr* 49(1):141–161
- Holte J, Talley LD, Gilson J, Roemmich D (2017) An Argo mixed layer climatology and database. *Geophys Res Lett* 44:5618–5626. <https://doi.org/10.1002/2017GL073426>
- Jesús González-Alemán J, Evans JL, Kowaleski AM, Ángel Gaertner M (2018) Factors affecting the structural evolution and predictability of the tropical transition of Hurricane Alex (2016). In EGU General Assembly Conference Abstracts (p. 475).
- Kalnay E, Kanamitsu M, Kistler R, Collins W, Deaven D, Gandin L, Zhu Y (1996) The NCEP/NCAR 40-year reanalysis project. *Bull Am Meteor Soc* 77(3):437–472
- Kanzow T, Johnson HL, Marshall DP, Hirschi JJM, Mujahid A, Bryden HL, Johns WE (2009) Basin-wide integrated volume transports in an eddy-filled ocean. *J Phys*
- Knapp KR, Kruk MC, Levinson DH, Diamond HJ, Neumann CJ (2010). The international best track archive for climate stewardship (IBTrACS) unifying tropical cyclone data. *Bull Am Meteorol Soc* 91(3): 363–376.
- Knapp KR, Diamond HJ, Kossin JP, Kruk M C, Schreck CJ (2018) International Best Track Archive for Climate Stewardship (IBTrACS) Project, Version 4.[WP, NP, NA, SI, NI, SP].
- Kossin JP, Knapp KR, Vimont DJ, Murnane RJ, Harper BA (2007) A globally consistent reanalysis of hurricane variability and trends. *Geophys Res Lett* 34(4)
- Kossin JP, Camargo SJ, Sitkowski M (2010) Climate modulation of North Atlantic hurricane tracks. *J Clim* 23(11):3057–3076
- Mainelli M, DeMaria M, Shay LK, Goni G (2008) Application of oceanic heat content estimation to operational forecasting of recent Atlantic category 5 hurricanes. *Weather Forecast* 23(1):3–16
- Mann ME, Steinman BA, Brouillette DJ, Miller SK (2021) Multidecadal climate oscillations during the past millennium driven by volcanic forcing. *Science* 371(6533):1014–1019
- McTaggart-Cowan R, Davies EL, Fairman JG Jr, Galarneau TJ Jr, Schultz DM (2015) Revisiting the 26.5° C sea surface temperature threshold for tropical cyclone development. *Bull Amer Meteor Soc* 96(11):1929–1943
- NOAA National Centers for Environmental Information (NCEI) U.S. Billion-Dollar Weather and Climate Disasters (2020). <https://www.ncdc.noaa.gov/billions/>, <https://doi.org/10.25921/stkw-7w73>
- Pasch RJ, Avila LA, Guiney JL (2001) Atlantic Hurricane Season of 1998. *Mon Wea Rev* 129:3085–3123
- Shapiro LJ, Goldenberg SB (1998) Atlantic sea surface temperatures and tropical cyclone formation. *J Clim* 11(4):578–590
- Smeed DA, Josey SA, Beaulieu C, Johns WE, Moat BI, Frajka-Williams E, McCarthy GD (2018) The North Atlantic Ocean is in a state of reduced overturning. *Geophys Res Lett* 45(3):1527–1533
- Walín G (1982) On the relation between sea-surface heat flow and thermal circulation in the ocean. *Tellus* 34:187–195
- Walín G (1982) On the relation between sea-surface heat flow and thermal circulation in the ocean. *Tellus*, 34(2): 187–195.
- Walín G (1982) On the relation between sea-surface heat flow and thermal circulation in the ocean. *Tellus* 34(2): 187–195.
- Wang C, Liu H, Lee SK, Atlas R (2011) Impact of the Atlantic warm pool on United States landfalling hurricanes. *Geophys Res Lett* 38(19).
- Wang C, Dong S, Evan AT, Foltz GR, Lee SK (2012) Multidecadal covariability of North Atlantic sea surface temperature, African dust, Sahel rainfall, and Atlantic hurricanes. *J Clim* 25(15):5404–5415.
- Watanabe M, Tatebe H (2019) Reconciling roles of sulphate aerosol forcing and internal variability in Atlantic multidecadal climate changes. *Clim Dyn* 53(7):4651–4665
- Zhang, R., & Delworth, T. L. (2006). Impact of Atlantic multidecadal oscillations on India/Sahel rainfall and Atlantic hurricanes. *Geophysical Research Letters*, 33(17).
- Zhang R, Sutton R, Danabasoglu G, Kwon Y-O, Marsh R, Yeager SG, Amrhein DE, Little CM (2019) A review of the role of the Atlantic meridional overturning circulation in Atlantic multidecadal variability and associated climate impacts. *Rev Geophys* 57. <https://doi.org/10.1029/2019RG000644>

**Publisher's Note** Springer Nature remains neutral with regard to jurisdictional claims in published maps and institutional affiliations.